AJNR

Physiologic intracranial calcification with hyperintensity on MR imaging: case report and experimental model.

L A Dell, M S Brown, W W Orrison, C G Eckel and N A Matwiyoff

AJNR Am J Neuroradiol 1988, 9 (6) 1145-1148
http://www.ajnr.org/content/9/6/1145

Physiologic Intracranial Calcification with Hyperintensity on MR Imaging: Case Report and Experimental Model

Lance A. Dell[1,2]
Mark S. Brown[1,3]
William W. Orrison[1,2,4]
Christopher G. Eckel[1,2]
Nicholas A. Matwiyoff[1-3]

CT and MR imaging showed basal ganglia calcification that appeared as high signal intensity on T1-weighted images of a patient with pseudohypoparathyroidism. MR imaging of an experimental model of calcium phosphate suspensions showed a signal similar to that seen in the patient. Additionally, T1 and T2 relaxation times of the solutions were measured and showed decreases in both parameters with increasing calcium phosphate concentrations.

Intracranial calcification can appear as high signal intensity on T1-weighted images. An experimental model shows that the calcium salt decreases the T1 of surrounding water. Therefore, calcium, and possibly other elements, may induce paramagnetic susceptibility effects.

Physiologic intracranial calcification is a relatively common finding, and its appearance on CT scans is well-known [1]. MR imaging of calcification has also been documented with a range of signal characteristics [2, 3]. We have studied a case of basal calcification having the typical CT attenuation and a previously unreported MR appearance of hyperintensity on T1-weighted images. An experimental model of aqueous calcium phosphate suspensions was developed to simulate this finding.

Subjects and Methods

An 18-year-old woman with a known history of pseudohypoparathyroidism, on calcium and vitamin D supplements, was seen in the emergency room after sustaining head trauma. A noninfused cranial CT scan at 10-mm slice thickness was obtained.* This was followed by MR imaging in a 1.5-T superconducting magnet.† T1-weighted spin-echo (SE) images were obtained with 600, 1500/20 (TRs/TE) and proton density and T2-weighted SE images were obtained with 2500/30, 80. Gradient refocused imaging (GRASS) was also performed with 75, 50/25 and a flip angle of 20°. Images were obtained at 3–5-mm slice thickness in sagittal, axial, and coronal planes. Follow-up imaging was performed at 2, 7, and 9 weeks after trauma.

An experimental phantom consisting of five tubes with different amounts of calcium phosphate in water was also imaged using the same pulse sequences (T1, proton density, T2, GRASS) as were used in patient imaging. The phantom was prepared by placing weighed amounts of $Ca(H_2PO_4)_2{*}H_2O$ (Reagent grade, Baker) in 50-ml plastic centrifuge tubes and then adding deionized, distilled H_2O. Concentrations used were 0.5, 1.0, 1.5, and 3.5 g $Ca(H_2PO_4)_2{*}H_2O$ per milliliter of water; one tube contained only water.

Prior to imaging, each tube was thoroughly shaken and then placed vertically in a linear arrangement using a styrofoam holder. Sagittal cuts were taken on the phantom in order to view the complete environment in each of the five tubes simultaneously. T1 measurements were obtained using partial saturation with eight TR values of 50–6000 and TE of 20. T2 was measured by using a multiecho sequence with eight echoes (2500/20–100). The values of several regions of interest were computed using T1 and T2 fitting routines available in the CLIPS utility of the GE software.

* GE 9800, General Electric Medical Systems, Waukesha, WI.
† GE, General Electric Model Systems, Waukesha, WI.

Received November 23, 1987; accepted after revision March 8, 1988.

[1] Center for Non-Invasive Diagnosis, University of New Mexico, School of Medicine, Albuquerque, NM 87131. Address reprint requests to L. A. Dell, Department of Radiology, San Juan Regional Hospital, 801 W. Maple, Farmington, NM 87401.

[2] Department of Radiology, University of New Mexico, School of Medicine, Albuquerque, NM 87131.

[3] Department of Cell Biology, University of New Mexico, School of Medicine, Albuquerque, NM 87131.

[4] Department of Neurology, University of New Mexico, School of Medicine, Albuquerque, NM 87131.

AJNR 9:1145–1148, November/December 1988
0195–6108/88/0906–1145

Results

The CT images showed high attenuation characteristic of calcification in the basal ganglia bilaterally, as well as in the frontal, temporal, and parietal lobes (Fig. 1A). In T1-weighted MR images (600/20) high signal was present in the basal ganglia, with other areas of high CT attenuation appearing iso- to hypointense (Fig. 1B). In relatively T1-weighted images (1500/20), the basal ganglia remained hyperintense with a slight increase in surrounding tissue signal (Fig. 1C). T2-weighted images showed the basal ganglia to be iso- to hypointense with no significant change in appearance of other areas of apparent calcification (Fig. 1D). In the GRASS images, the basal ganglia exhibited varying degrees of hypointensity (Fig. 1E). In the initial MR examination, there was evidence of acute hemorrhage within the right mastoid air cells. Subsequent imaging showed no change in appearance of the basal ganglia and typical changes of clot maturation were seen in the right mastoid.

Visual inspection and the water proton images of the phantoms containing aqueous suspensions of insoluble calcium phosphate showed that the salt settles into layers. The gravimetric settling of particles of different sizes results in a colloidal suspension of the small particles at the top of the tubes and large crystals at the bottom of the tubes. It can be seen that the signal characteristics of the upper portions of the tubes are similar to those seen in the patient (Fig. 2A). In the T1-weighted image (Fig. 2A), the water protons of the suspensions of small crystals exhibited high signal intensity whereas those of the larger crystals at the bottom of the tubes exhibited lower signal intensity. Part of this difference can be attributed to proton density differences between the colloidally suspended salt crystals toward the tops of the tubes and the more settled, larger crystals with less water at the bottoms of the tubes. Quantitatively, the T1 and T2 values were quite revealing (Figs. 2A and 2B). As would be expected, both T1 and T2 in solutions containing the calcium salt were significantly reduced relative to pure water. However, T1

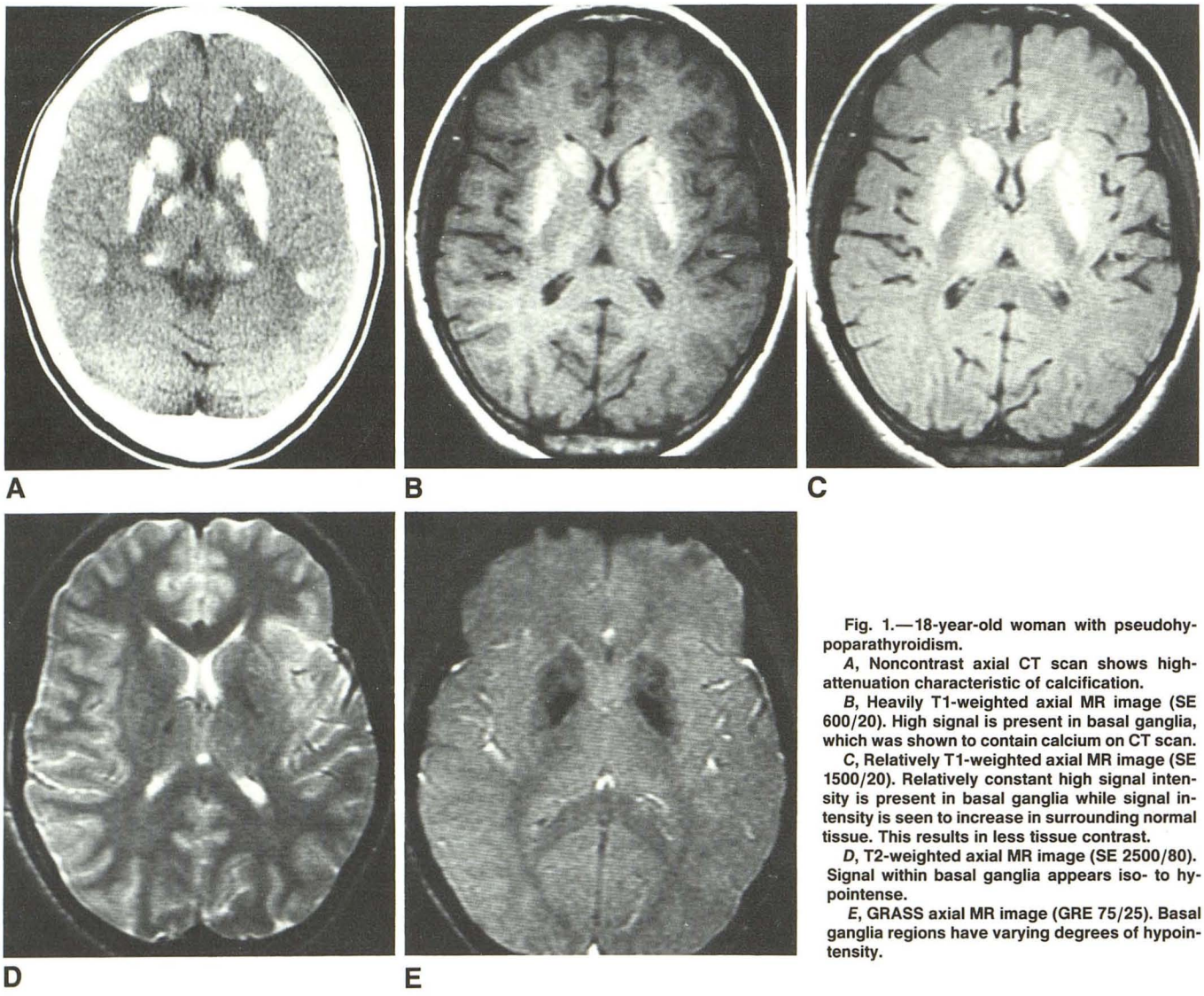

Fig. 1.—18-year-old woman with pseudohypoparathyroidism.

***A*, Noncontrast axial CT scan shows high-attenuation characteristic of calcification.**

***B*, Heavily T1-weighted axial MR image (SE 600/20). High signal is present in basal ganglia, which was shown to contain calcium on CT scan.**

***C*, Relatively T1-weighted axial MR image (SE 1500/20). Relatively constant high signal intensity is present in basal ganglia while signal intensity is seen to increase in surrounding normal tissue. This results in less tissue contrast.**

***D*, T2-weighted axial MR image (SE 2500/80). Signal within basal ganglia appears iso- to hypointense.**

***E*, GRASS axial MR image (GRE 75/25). Basal ganglia regions have varying degrees of hypointensity.**

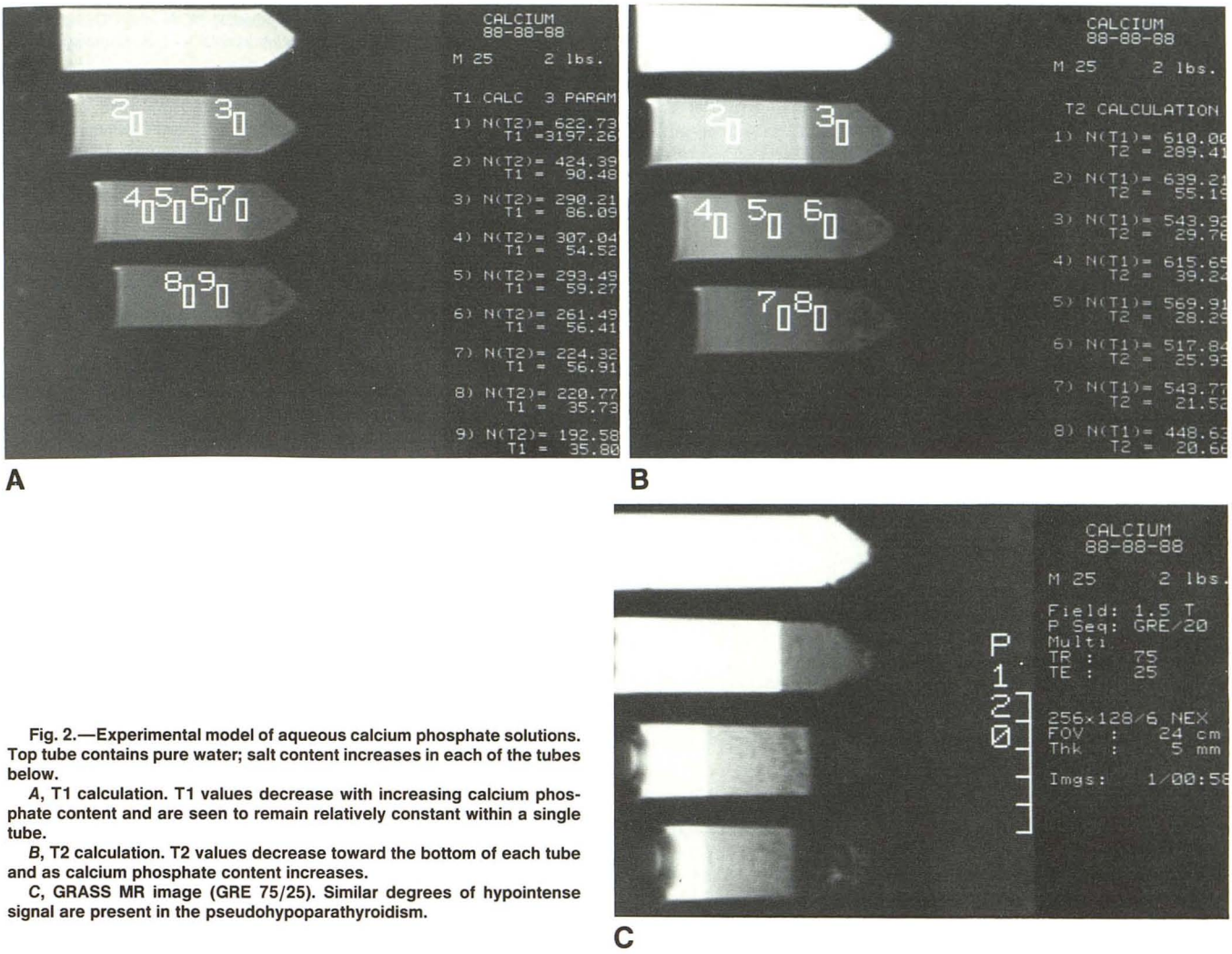

Fig. 2.—Experimental model of aqueous calcium phosphate solutions. Top tube contains pure water; salt content increases in each of the tubes below.

***A*, T1 calculation. T1 values decrease with increasing calcium phosphate content and are seen to remain relatively constant within a single tube.**

***B*, T2 calculation. T2 values decrease toward the bottom of each tube and as calcium phosphate content increases.**

***C*, GRASS MR image (GRE 75/25). Similar degrees of hypointense signal are present in the pseudohypoparathyroidism.**

remained relatively constant throughout the different layers in a single tube, while T2 decreases as the degree of settling increased. The lower the T2, the darker the area appeared in the T1-weighted image. GRASS imaging of these tubes revealed varying degrees of hypointense signal, as was present in the patient (Fig. 2C).

Discussion

The previously reported MR appearance of intracranial calcification is varied, ranging from markedly hypointense to signal dampening, to imperceptible [2–7]; however, the observation of high signal intensity in heavily T1-weighted images has not been described. In this patient with a medical condition known to predispose to basal calcification and characteristic high attenuation in the basal ganglia by CT, it appears that calcium deposits in this area have the same effect on surrounding water as was demonstrated to occur in vitro; i.e., a shortening of the relaxation times. If this physiologic calcification exhibits a reduction of water T1 as large as was seen in the experimental model, signal intensity will be unaffected by short TR values [intensity = $I_o(1-e^{-TR/T1})$ = $I_o(1-e^{-600/90})$ = I_o], where TR = repetition time and T1 = T1 of imaged tissue. Conversely, more normal tissue adjacent to the regions of calcification have higher T1 values and will exhibit a marked reduction in signal intensity [intensity = $I_o(1-e^{-600/90})$ = 0.5 I_o]. The 600/20 and 1500/20 images demonstrated contrast consistent with these expectations. The basal ganglia remained relatively bright in both images; however, the contrast with surrounding tissue was lower in the 1500/20 image due to greater intensity from the surrounding tissue with its longer T1.

The results from the phantom also show that T2 is affected quite strongly, and in some way this seems to be associated with the degree of settling of salt. Thus, in addition to proton density, the T1 and T2 values of water associated with calcium deposits may strongly affect the contrast of such areas in MR.

It has been shown previously that physiologic calcifications contain varying amounts of iron [8] and possibly paramagnetic metals such as manganese. The presence of such materials could mimic the T1 and T2 changes observed in the phantom, and paramagnetic contribution in the patient cannot be ruled

out. The results on the phantoms show, however, that it is not necessary to invoke paramagnetic materials in order to explain the appearance of the calcified region. Other more likely contributions are hydration effects and magnetic susceptibility gradient across the areas of calcification or along the axis of the tube in the experimental model. These findings suggest that the appearance of calcified regions in tissue imaged with MR can vary greatly, depending on the actual structure and degree of calcification.

REFERENCES

1. Norman D, Diamond C, Boyd D. Relative detectability of intracranial calcifications on computer tomography and skull radiography. *J Comput Assist Tomogr* **1978**; 2:62–64
2. Holland BA, Kucharczyk W, Brant-Zawadzki M, Norman D, Haas DK, Harper, PS. MR imaging of calcified intracranial lesions. *Radiology* **1985**; 157:353–356
3. Oot RF, New PF, Pile-Spellman J, Rosen BR, Shoukimas GM, Davis KR. The detection of intracranial calcifications by MR. *AJNR* **1986**; 7:801–809
4. Brant-Zawadzki M, Davis PL, Crooks LE, et al. NMR demonstration of cerebral abnormalities: comparison with CT. *AJNR* **1983**; 4:1013–1026, *AJR* **1983**; 140:847–854
5. Kjos BO, Brant-Zawadzki M, Kucharczyk W, Kelly WM, Normal C, Newton TH. Cystic intracranial lesions: magnetic resonance imaging. *Radiology* **1985**; 155:363–369
6. Kucharczyk W, Lemme-Pleghos L, Uske A, Brant-Zawadzki M, Dooms G, Norman D. Intracranial vascular malformations: MR and CT imaging. *Radiology* **1985**; 156:383–389
7. Zimmerman RD, Fleming CA, Saint-Louis LA, Manning JJ, Deck MDF. Magnetic resonance imaging of meningiomas. *AJNR* **1985**; 6:149–157
8. Lowenthal A, Bruyn GW. Calcification of the striopallidodentate systems. In: Vinken PJ, Bruyn GW, eds. *Handbook of clinical neurology*, vol. 6. Amsterdam: North Holland, **1968**:203–723